

Effect of Mesh Quality on the Numerical Solution of the Solidification of Pure Metal

T. Skrzypczak ^{a,*}, E. Węgrzyn-Skrzypczak ^b

^a Institute of Mechanics and Machine Design, Faculty of Mechanical Engineering and Computer Science, Czestochowa University of Technology, Dąbrowskiego 73, 42-200 Czestochowa, Poland

^b Institute of Mathematics, Faculty of Mechanical Engineering and Computer Science, Czestochowa University of Technology, Armii Krajowej 21, 42-200 Czestochowa, Poland

*Corresponding author. E-mail address: skrzyp@imipkm.pcz.pl

Received 25.06.2013; accepted in revised form 09.09.2013

Abstract

The paper presents a method of mathematical and numerical modelling of directional solidification process of pure metal in the two-dimensional region. In this case, the thermal conditions associated with the process favours the occurrence of sharp solidification front. The mathematical description of the process is based on the Stefan formulation with appropriate continuity conditions on the solid-liquid interface. The numerical model is based on the finite element method (FEM). The calculations were made on a fixed mesh with diffused solidification front to avoid the difficulties associated with the discontinuity. Temporary position of the interface was calculated with the use of the level set method (LSM). Effect of the quality of the spatial discretization on the accuracy of numerical solution was investigated. Obtained results of the temporary front position were compared with the analytical solution. The correlation between the quality of the spatial discretization and the accuracy of the results was observed. Methods used in the work had significant impact on the computation time and helped avoid the explicit consideration of discontinuity of heat flux on the front.

Keywords: Solidification process, Application of information technology to the foundry industry, Pure metal, Stefan problem, Finite element method

1. Introduction

In the case of alloy solidification front often loses stability which is caused by the phenomenon called solutal undercooling [1, 2]. This phenomenon is often neglected but its effect is indirectly adopted in the models based on the solidification between the solidus and liquidus temperatures [3, 4]. During solidification of pure metal interface stability depends on the direction of heat flow [5]. In the case of directional solidification temperature of the liquid always increases ahead of the interface, therefore the heat flow direction is opposite that of solid phase growth. When a small perturbation appears on a smooth interface, the heat flow through its tip increases and finally it melts back.

Such process stabilizes the interface thus it remains sharp until the end of solidification. From this point of view directional solidification of a pure metal belongs to the group of Stefan problems which describe various phenomena that take place with the existence of a sharp internal interface.

Numerical methods based on the Stefan formulation for solving solidification or melting processes, which can be found in the literature can be classified into following groups:

- methods based on the diffused front. Solidification at a constant temperature is replaced by a process which takes place in a narrow temperature range [6] or temperature is constant but the front is diffused [7].

- methods based on the adaptation of mesh where the edges of the finite elements are matched to the shape of the moving interface [8];
- methods based on discontinuous approximation functions in finite elements containing solidification interface. In this approach the finite element mesh does not change with time [9, 10];

Tracking solidification front is a significant challenge for anyone who create numerical models for Stefan problems. It is obvious, that the temporary position of the front can be arbitrarily positioned between the nodes, which leads to considerable difficulties in determining the temperature along it. LSM is a powerful and widely used method for the propagation of internal interfaces during solidification of pure metals and alloys in the micro-scale, two-phase flows, cracks propagation, computer vision, images processing, etc. LSM was first applied to Stefan problems in [11]. Other methods, such as cellular automata are also used for this purpose [12].

2. Governing equations

Considered region consists of solid Ω_S and liquid Ω_L sub-regions (Fig. 1) separated by solidification front Γ_{int} .

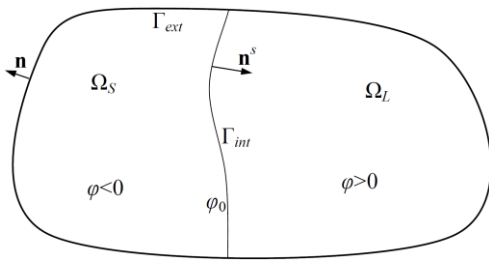


Fig. 1. Solidifying area contains moving internal boundary Γ_{int}

Heat transport in solidifying area is described by the equation of heat conduction

$$\frac{\partial}{\partial x} \left(\lambda \frac{\partial T}{\partial x} \right) + \frac{\partial}{\partial y} \left(\lambda \frac{\partial T}{\partial y} \right) - c\rho \frac{\partial T}{\partial t} = 0 \quad (1)$$

Position of the front is determined using following equation

$$u_x \frac{\partial \varphi}{\partial x} + u_y \frac{\partial \varphi}{\partial y} + \frac{\partial \varphi}{\partial t} = 0 \quad (2)$$

Variable φ appearing in (2) is called the distance function. It measures the shortest distance between any point in the area and solidification interface Γ_{int} . It is a function of position and time satisfying the following condition

$$\varphi(\mathbf{x}, t) = \min_{\bar{\mathbf{x}} \in \Gamma_{int}} \left\| \mathbf{x} - \bar{\mathbf{x}} \right\| \operatorname{sgn} \left[\mathbf{n}^s \cdot (\mathbf{x} - \bar{\mathbf{x}}) \right] \quad (3)$$

Equations (1-2) are supplemented by following boundary (4), initial (5) and continuity conditions (6-7)

$$T|_{\Gamma_{ext}} = T_b, \quad -\lambda \frac{\partial T}{\partial n} \Big|_{\Gamma_{ext}} = q_b \quad (4)$$

$$T|_{t=0} = T_0, \quad \varphi|_{t=0} = \varphi_0 \quad (5)$$

$$T^s \Big|_{\Gamma_{int}} = T^l \Big|_{\Gamma_{int}} = T_M \quad (6)$$

$$\lambda_s \frac{\partial T^s}{\partial n^s} \Big|_{\Gamma_{int}} - \lambda_l \frac{\partial T^l}{\partial n^s} \Big|_{\Gamma_{int}} = \rho_s L |\mathbf{u}| \quad (7)$$

where $T=T(x, y, t)$ is the temperature [K], $\lambda=\lambda(T)$ - coefficient of thermal conductivity [$\text{J s}^{-1} \text{m}^{-1} \text{K}^{-1}$], $c=c(T)$ - specific heat [$\text{J kg}^{-1} \text{K}^{-1}$], $\rho=\rho(T)$ - density [kg m^{-3}], t - time [s], x, y - Cartesian coordinates [m], $\varphi=\varphi(x, y, t)$ is a signed distance function [m], u_x, u_y - components of the interface velocity vector [m s^{-1}], $T_0=T_0(x, y)$ is the initial temperature [K], $\varphi_0 = \varphi_0(x, y)$ - the initial position of solidification front [m], $T_b=T_b(x, y)$ - a given boundary temperature [K], Γ_{ext} - the external boundary, n - the direction of the vector pointing outwards Γ_{ext} , n^s - the direction of the vector pointing outwards Γ_{int} , T_M - melting (solidification) temperature [K], q - heat flux normal to the external boundary Γ_{ext} [$\text{J s}^{-1} \text{m}^{-2}$], \mathbf{u} - velocity of the solidification front, L - latent heat of solidification [J kg^{-1}], s, l - means a solid or liquid.

2.1. Numerical model

According to the weighted residuals method, equations (1-2) are multiplied by a weight function $w=w(x, y)$ and integrated around the entire region

$$\iint_{\Omega} w \left[\frac{\partial}{\partial x} \left(\lambda \frac{\partial T}{\partial x} \right) + \frac{\partial}{\partial y} \left(\lambda \frac{\partial T}{\partial y} \right) - c\rho \frac{\partial T}{\partial t} \right] dx dy = 0 \quad (8)$$

$$\iint_{\Omega} w \left[u_x \frac{\partial \varphi}{\partial x} + u_y \frac{\partial \varphi}{\partial y} + \frac{\partial \varphi}{\partial t} \right] dx dy = 0 \quad (9)$$

After spatial discretization using standard Galerkin formulation and time discretization based on the forward Euler method the following global finite element equations are obtained

$$\mathbf{T}^f = \Delta t \mathbf{M}_T^{-1} \left[\mathbf{B}_T + \left(\frac{1}{\Delta t} \mathbf{M}_T - \mathbf{K}_T \right) \mathbf{T}^{f-1} \right] \quad (10)$$

$$\boldsymbol{\varphi}^f = \Delta t \mathbf{M}_{\varphi}^{-1} \left(\frac{1}{\Delta t} \mathbf{M}_{\varphi} - \mathbf{A}_{\varphi} \right) \boldsymbol{\varphi}^{f-1} \quad (11)$$

where \mathbf{K}_T is the thermal conductivity matrix, \mathbf{M}_T - heat capacity matrix, \mathbf{B}_T - vector associated with the boundary conditions, \mathbf{A}_{φ} - advection matrix, \mathbf{M}_{φ} - mass matrix, Δt - time step [s], $f-1, f$ - time level.

3. Numerical examples

The main purpose of the numerical simulations was to examine the impact of the quality of the spatial discretization on the accuracy of the method in modeling of the solidification process of pure copper. Adopted material properties [13] are summarized in Table 1.

Table 1. Material properties of pure copper used in the model

Material property	Solid	Liquid
ρ [kg m ⁻³]	8920.0	8300.0
λ [J s ⁻¹ m ⁻¹ K ⁻¹]	330.0	250.0
c [J kg ⁻¹ K ⁻¹]	420.0	544.0

One series of tests were carried out using three types of meshes, and the calculated temporary position of the front was compared with analytical solution [14], where the change in the position of the front in time was described using the following equation

$$X(t) = 2k_0\sqrt{\alpha_l t} \quad (12)$$

where k_0 is a root of the transcendental equation

$$\frac{St_l}{e^{k^2} \operatorname{erf}(k)} - \frac{St_s}{ve^{\nu^2 k^2} \operatorname{erfc}(\nu k)} - k\sqrt{\pi} = 0 \quad (13)$$

The coefficients in the above equation were defined as follows

$$\alpha_s = \frac{\lambda_s}{\rho_s c_s}, \quad \alpha_l = \frac{\lambda_l}{\rho_l c_l}, \quad \nu = \sqrt{\frac{\alpha_l}{\alpha_s}} \quad (14)$$

$$St_s = \frac{c_s(T_0 - T_M)}{L}, \quad St_l = \frac{c_s(T_M - T_b)}{L} \quad (15)$$

where α_s , α_l are the coefficients of thermal diffusivity in a solid and liquid phase [m² s⁻¹] and St_s , St_l are Stefan numbers in the solid and liquid [-].

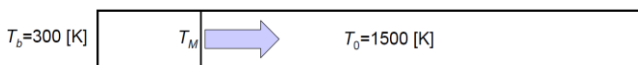


Fig. 2. Sketch of a test task

The rectangular area measuring 0.02x0.2 [m], with the initial and boundary conditions are shown in Fig. 2. Adopted conditioning enabled the comparison of results obtained with the solution of the equation (12).

Calculations were performed for meshes with an average element size $h^{(e)} = 2e-3, 1e-3, 5e-4$ [m] corresponding to 1295, 4694, 18645 nodes. Time step was constant and equal to 1e-4 [s]. Summary of results for $t = 1, 2, 5, 10, 20, 50$ [s] and their comparison with the analytical solution (Fig. 3) clearly shows the good accuracy of the applied model. The quality of the spatial

discretization affected a little the accuracy of the calculations because of simple shape of the solidification front.

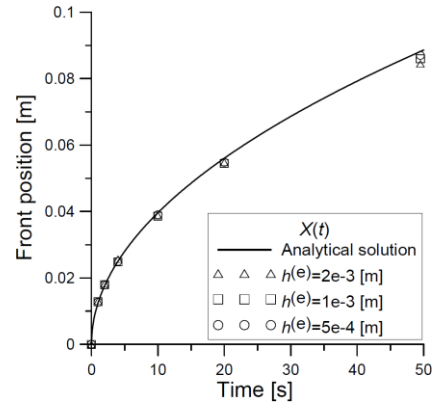


Fig. 3. Front position according to time

A second series of tests were conducted to determine the effect of the quality of the spatial discretization on the accuracy of propagation of the curved front. The shape of the area 0.1x0.1 [m] and the boundary and initial conditions are shown in Fig. 4.

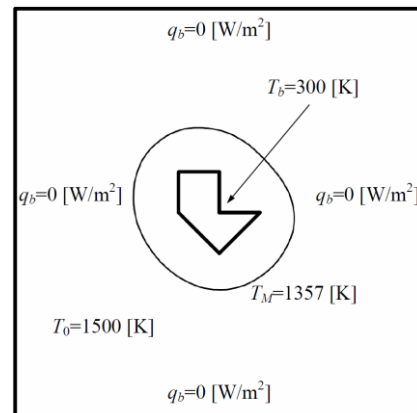


Fig. 4. Test of the curved front propagation

In this case calculations were carried out with the use of meshes with an average element size $h^{(e)} = 5e-4, 3.75e-4, 2.5e-4$ [m] corresponding to 45852, 80858, 183614 nodes. Time step was equal to 1e-4 [s] for low and medium quality meshes and 5e-5 [s] for the best one. Fig. 5 shows the results of the calculations. Presented contours indicates temporary positions of the solidification front. Dashed line corresponds to the worst quality mesh. Thin continuous line relates to the average quality of the mesh and the thick continuous line shows the results for the most accurate spatial discretization. An analysis of the results which are obtained for different mesh qualities shows that a systematic error is introduced in the approximation of the absolute value of the distance function gradient. This effect is called "area loss" and is widely described in the literature [15].

Front position calculated on the most sparse mesh differs from the accurate position. Improving mesh quality above particular level is useless due to the lack of significant improvement in accuracy. Optimal element size for presented task is 3.75e-4 [m].

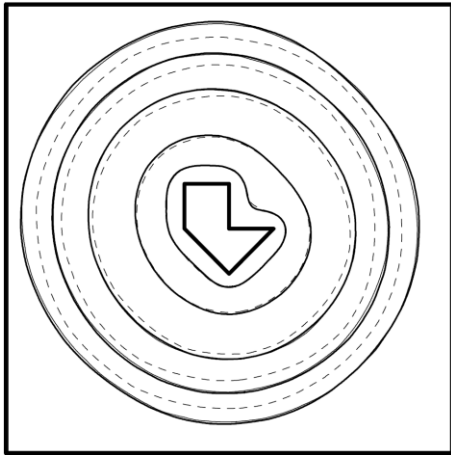


Fig. 5. Temporary positions of the front for different mesh qualities after 0.1, 1, 5, 10, 15 [s]

4. Conclusions

Described mathematical and numerical models of solidification process of pure copper shows the possibility of introducing the continuity conditions at the sharp solidification front in the diffused form. The presented front tracking technique proves its usefulness in solving the problems with moving internal boundaries. Comparison of the results for meshes of varying quality, and the fronts of different shapes shows the phenomenon of "area loss" and how to minimize its impact on the accuracy of numerical calculations.

References

- [1] Kapturkiewicz, W., Burbelko, A. A. & Fraś, E. (2008). Mathematical and numerical model of directional solidification including initial and terminal transients of the process. *Archives of Foundry Engineering*. 8(4), 65-70.
- [2] Skrzypczak, T. & Węgrzyn-Skrzypczak, E. (2008). Numerical modelling of the binary alloys solidification with solutal undercooling. *Archives of Foundry Engineering*. 8(1), 299-302.
- [3] Sowa, L. (2010). Numerical analysis of the thermal and fluid flow phenomena of the fluidity test. *Archives of Foundry Engineering*. 10(1), 157-160.
- [4] Sowa, L. (2011). Effect of nozzle outlet angle on flow and temperature field in a slab continuous casting mould. *Archives of Foundry Engineering*. 11(2), 199-202.
- [5] Kurz, W., Fisher, D. J. (1998). *Fundamentals of Solidification*. (4th ed.). London-Paris: Trans. Tech. Publ.
- [6] Rolph, D. & Bathe, K. J. (1982). An efficient algorithm for analysis of nonlinear heat transfer with phase change. *International Journal of Numerical Methods in Engineering*. 18(1), 119-134. DOI: 10.1002/nme.1620180111.
- [7] Skrzypczak, T. (2012). Sharp interface numerical modeling of solidification process of pure metal. *Archives of Metallurgy and Materials*. 57(4), 1189-1199. DOI: 10.2478/v10172-012-0133-1.
- [8] Bell, G. E. (1978). A refinement of the heat balance integral method applied to a melting problem. *International Journal of Heat and Mass Transfer*. 21(11), 1357-1362. DOI: [http://dx.doi.org/10.1016/0017-9310\(78\)90198-9](http://dx.doi.org/10.1016/0017-9310(78)90198-9).
- [9] Chessa, J., Smolinski, P. & Belytschko, T. (2002). The extended finite element method (XFEM) for solidification problems. *International Journal for Numerical Methods in Engineering*. 53(8), 1959-1977. DOI: 10.1002/nme.386.
- [10] Skrzypczak, T., Węgrzyn-Skrzypczak, E. (2012). Mathematical and numerical model of solidification process of pure metals. *International Journal of Heat and Mass Transfer*. 55(15-16), 4276-4284. DOI: <http://dx.doi.org/10.1016/j.ijheatmasstransfer.2012.03.070>.
- [11] Chen, S., Merriman, B., Osher, S. & Smereka, P. (1997). A simple level set method for solving Stefan problems. *Journal of Computational Physics*. 135(1), 8-29. DOI: <http://dx.doi.org/10.1006/jcph.1997.5721>.
- [12] Burbelko, A. A., Kapturkiewicz, W., Gurgul, D. (2007). Computation of interface curvature in modelling of solidification by the method of cellular automaton. *Archives of Foundry Engineering*. 7(1), 41-46.
- [13] Mochnecki, B., Suchy, S. J. (1995). Numerical methods in computations of foundry processes. Polish Foundrymen's Technical Association, Kraków.
- [14] Boucíguez, A. C., Lozano, R. F. & Lara, M. A. (2007). About the exact solution in two-phase Stefan problem. *Thermal Engineering*. 6(2), 70-75.
- [15] Peng, D., Merriman, B., Osher, S. & Zhao, H. (1999). A PDE-based fast local level set method. *Journal of Computational Physics*. 155, 410-438. DOI: <http://dx.doi.org/10.1006/jcph.1999.6345>.